

# Determination of Prostate-Specific Antigen Via The Assembly of a Two-Dimensional Nanoplatform

**Junjie Chen**

South China Normal University

**Xiangqian Li**

South China Normal University

**Xiaoqi Yu**

Guangzhou Reagent Environmental Technology

**Qianming Wang** (✉ [rareearth@126.com](mailto:rareearth@126.com))

South China Normal University <https://orcid.org/0000-0003-2795-6056>

---

## Research Article

**Keywords:** CoOOH nanosheets, Prostate-specific antigen, Fluorescent probe

**Posted Date:** September 20th, 2021

**DOI:** <https://doi.org/10.21203/rs.3.rs-869977/v1>

**License:**  This work is licensed under a Creative Commons Attribution 4.0 International License.

[Read Full License](#)

---

**Version of Record:** A version of this preprint was published at Journal of Nanoparticle Research on April 18th, 2022. See the published version at <https://doi.org/10.1007/s11051-022-05437-z>.

## Abstract

Two-dimensional platforms with favorable features are highly expected for diverse application. In this work, we report a highly sensitive and selective “turn-on” fluorescent nanoprobe for prostate-specific antigen (PSA) detection base on cobalt oxyhydroxide nanosheets (CoOOH NSs). CoOOH NSs are employed as the suitable sensing hosts, in which fluorescein amidite-(abbreviated as FAM) labeled aptamer probe (PA) has been adsorbed on nanosheets. Energy transfer between substrate and optical species has switched off the fluorescence of PA. The strong affinity of PA to the target PSA induces the formation of a rigid aptamer structure and the integration with the CoOOH NSs has been drastically affected. The recognition process has been followed by the release of the aptamer probe PA from the nanosheet surface and the green luminescence has been recovered. The dynamic nano-sensor exhibits highly sensitive and accurate analytical performance toward PSA with a linear detection range from 0.1 to 5 nM and a detection limit of 56.1 pM. Therefore, a simple and efficient sensing platform for the detection of prostate cancer can be established.

## Introduction

Cancer refers to disease that involves abnormal cell growth and may affect various parts of the body. Prostate cancer is one of the main cancer types which will be harmful to the health. Prostate-specific antigen (PSA) is a single-chain polypeptide containing 237 amino acids and is the most sensitive biomarker for prostate cancer [1–3]. Therefore, it is an urgent and important task to develop biomarkers for detecting prostate cancer with higher sensitivity. So far, a variety of analytical techniques have been used to detect PSA, such as radioimmunoassay, mass spectrometry immunoassay, enzyme-linked immunosorbent assay, colorimetric analysis, electrochemical methods, polymerase chain reaction and surface enhancement Raman analysis [4–9]. However, these methods require expensive apparatus and complicated pretreatment procedures. Determination process with facile steps would be warmly welcome. From last decade, fluorescence-based technology has attracted widespread attention due to its high sensitivity, simplicity and stability [10–12]. As for the structure, 2D materials have generated significant interests in biological applications due to their unique properties such as large surface area, bio-compatibility, and low toxicity [13–15]. In particular, 2D nanosheets have been provided as the excellent platforms for the detection of DNA sequence. As a result, a variety of 2D nanosheets, including transition metal dichalcogenide, metal oxides, and carbon nanomaterials, have been developed to construct nano-fluorescence sensor for the DNA detection [16–20]. Therefore, in our present study, we employed a highly sensitive two-dimensional CoOOH nanosheets based PSA sensor via the transduction of optical signals and CoOOH NSs were played as the host for the sensing process.

The cobalt oxyhydroxide nanosheet has been developed as a novel transition metal-based oxide nanomaterial with regular hexagon and rigid two-dimensional structure [21–23]. Therefore, the structure possesses similar features as some reported 2D nanosheets, such as graphene oxide (GO), MoS<sub>2</sub>, WS<sub>2</sub>, MnO<sub>2</sub> and so on [24–28]. Most of them have been extensively used for biological applications owing to their quantum size properties and surface effects. Some of them were functionalized as powerful

quenchers not only for organic fluorescent dyes but also for some fluorescent nanoparticles such as up-conversion nanoparticles and quantum dots [29, 30]. Because of the quantities of hydroxyls on the CoOOH NSs surface, CoOOH NSs gave rise to excellent water solubility, good biocompatibility and large specific surface area, which would contribute to the potential uses in environmental or biological conditions [31, 32]. To our knowledge, the employment of CoOOH NSs as the biosensor platform for the detection of PSA has not been reported.

Herein, CoOOH NSs were used as the signal substrate and its microstructure was verified. It has been found that CoOOH NSs can selectively adsorb fluorescent dye FAM-labeled aptamers (PA) and act as an efficient fluorescent dye quencher. The binding of the aptamer to the target PSA induced a rigid aptamer structure which significantly changed the integration process with the CoOOH NSs. Accordingly, such recognition resulted in the release of the aptamer PA from the nanosheet surface and restored the quenched fluorescence (Scheme 1). Therefore, the assay could be considered as direct, simple, sensitive, selective and suitable for PSA detection. It can be expected that the CoOOH NSs nano-host strategy would provide possibility in the field of early clinical diagnosis.

## Experimental

### Materials

Cobalt(II) chloride hexahydrate ( $\text{CoCl}_2 \cdot 6\text{H}_2\text{O}$ ), sodium hydroxide (NaOH), Sodium hypochlorite (NaClO) and other reagents were obtained from Guangzhou Chemical Reagent Factory and used without further purification. Prostate-specific antigen (PSA) was obtained from Shanghai Linc-Bio Science Co. Ltd. (Shanghai, China). The stock solutions of oligonucleotides were prepared in Tris-HCl (10 mM, pH 7.4, containing 150 mM NaCl, 5 mM KCl, and 5 mM  $\text{MgCl}_2$ ). All oligonucleotides were synthesized and purified by Sangon Biotechnology Co., Ltd. (Shanghai, China). The corresponding sequences were as follows:

PSA aptamer (PA) 5'-/FAM/-TTATTAAAGCTGCCATCAAATAGC-3'

### Apparatus

Powder X-ray diffraction (PXRD) data were collected on a Bruker D8-ADVANCE X-ray diffractometer with Cu  $K\alpha$  radiation ( $\lambda = 1.5418 \text{ \AA}$ ) (Bruker, Germany). Transmission electron microscopy (TEM) images were obtained with a JEOL JEM-2100HR (Hitachi, Japan). The morphologies and structures of CoOOH NSs was examined by field emission scanning electron microscope (SEM, Sigma 500) equipped with an energy dispersive X-ray spectrum attachment (EDX Oxford Instruments Isis 300) (Zeiss, Germany). X-ray photoelectron spectroscopy (XPS) measurements were performed on a VG ESCALAB 220iXL surface analysis system. The zeta potential of CoOOH NSs was determined by Malvern Nano-ZS90 system (Malvern, United Kingdom). Fourier transform infrared (FT-IR) spectra was recorded on a Nicolet 6700 (Thermo, United States). Thermo gravimetric analysis (TGA) experiments were carried out using SII EXStar6000 TG/DTA6300 thermal analyzer from room temperature to 800 °C under an air atmosphere at

a heating rate of  $10\text{ }^{\circ}\text{C}\cdot\text{min}^{-1}$ . The UV-vis spectrum was obtained using a Shimadzu UV-2600 spectrophotometer (Shimadzu, Japan). Fluorescence measurements were conducted using a Hitachi F-7000 fluorescence spectrophotometer with a 150 W xenon lamp as a light source (Hitachi, Japan).

## Synthesis of CoOOH NSs

We have synthesized the CoOOH NSs following previous literature [33]. First, 1.25 mL 1 M NaOH was added into a glass vial with 5 mL 10 mM  $\text{CoCl}_2\cdot6\text{H}_2\text{O}$  and subjected to ultrasounds for one minute. Then the mixture was mixed with 0.25 mL 0.9 M NaClO followed by an ultrasound treatment for ten minutes. Subsequently the mixture was subjected to centrifugation and washed with water three times. Finally, the CoOOH NSs were dispersed in deionized water and stored at  $4\text{ }^{\circ}\text{C}$  for further use.

## Fluorescent sensing of PSA

In a typical PSA detection, the aptamer probe PA (50 nM) in 10 mM Tris-HCl buffer was incubated with different concentrations of PSA at  $37\text{ }^{\circ}\text{C}$  for 30 min. Then, the CoOOH NSs suspension (35  $\mu\text{g}/\text{mL}$ ) were added to the above mixed solution and incubated at room temperature for 10 min. The final concentration of PSA ranged from 0 to 100 nM. Finally, the sample was put into a fluorescence spectrometer and the fluorescence spectra were measured and collected by a fluorescence spectrophotometer excited at 495 nm. For comparison purpose, control experiments were performed by replacing PSA with other interfering analytes, such as  $\text{CaCl}_2$ ,  $\text{MgCl}_2$ ,  $\text{ZnCl}_2$ , bovine serum albumin (BSA), glutathione (GSH), L-cysteine (Cys), urea (UA), ascorbic acid (AA) and vitamin B1 (VB1).

## Results And Discussion

It has been reported that ultrathin nanosheets are regarded as the suitable units that could connect the microscopic property with excellent macroscopic features [34, 35]. In this study, the CoOOH nanosheets have been used as efficient quencher owing to optical absorption and high surface area. As the energy acceptor, ultrathin CoOOH NSs were synthesized by the previously reported method with slight modification. The structures of the CoOOH NSs were evaluated by X-ray powder diffraction (XRD). As is shown in Fig. 1A, the XRD pattern of CoOOH NSs possesses three representative peaks at 20.19, 38.95 and  $50.62^{\circ}$ , such signals can be indexed as (003), (012) and (015) planes of CoOOH NSs according to the standard JCPDS card (No. 73–0497). The intense and sharp diffraction peaks demonstrate that the product is well crystallized. The full-scan X-ray photo electron spectroscopy (XPS) of CoOOH NSs has been determined to explore their composition (Fig. 1B). Two peaks at 532.7 eV and 787.3 eV were attributed to O 1s and Co 2p, respectively. TEM images supported the existence of typical hexagon nanosheets morphology of CoOOH NSs (Fig. 1C). In addition, the major elemental analysis was demonstrated by Energy Dispersive Spectroscopy (EDS). The curve confirmed the presence of Co and O elements and the distribution has been given in Fig. 1D. Moreover, SEM images and the energy dispersive X-ray mapping results clearly proved the presence of Co and O elements (Fig. 2). The FT-IR spectrum of the CoOOH NSs is shown in Fig. S1. The broad band located at  $3415\text{ cm}^{-1}$  is attributed to the vibrations of free O-H from the surface of CoOOH NSs. Meanwhile, the peak at  $1635\text{ cm}^{-1}$  assigned to Co = O

double bond has been observed (32). Therefore, all above results verified that ultrathin CoOOH NSs were successfully fabricated. The zeta potential of the CoOOH NSs was 21.1 mV, showing the positive charge was found in the nanosheets (Fig. S2). The TGA curves revealed that the CoOOH NSs were thermally stable, less than 10 % of mass loss was observed even at temperature as high as 290 °C (Fig. S3).

To demonstrate the optical performance of the PSA sensor, the fluorescence quenching and subsequent recovery ability of PA were evaluated in the presence of CoOOH NSs and PSA. The FAM labeled aptamer (PA) was used as a probe to monitor PSA. The fluorescence quenching ability of CoOOH NSs was firstly investigated. As shown in Fig. 3A, with the increasing concentration of CoOOH NSs (from 0 to 35 µg/mL), the emission intensity of PA (50 nM) was gradually suppressed and finally almost completely quenched. Moreover, the fluorescence intensity was maintained stable within only 3 min, indicating the fast quenching of CoOOH NSs toward PA (Fig. S4). When PA was hybridized with excessive PSA, the PA/PSA duplex was formed and the quenched fluorescence of PA was recovered in the presence of CoOOH NSs (Fig. 3B). It is estimated that CoOOH NSs had weaker affinity to dsDNA than to ssDNA.

The UV-vis absorption spectrum of CoOOH NSs was explored (Fig. 4). It can be found that the absorption curve covers a wide range of wavelengths from ultraviolet light to visible region, which suggested that the CoOOH NSs can be considered as an ideal energy acceptor for diverse chromophores. The close proximity of the aptamer PA and CoOOH NSs has provided the possibility of the fluorescence resonance energy transfer (FRET) process from the excited FAM dye to the CoOOH NSs. The FRET channel mainly depended on the spectral overlap between the absorption spectrum of the energy acceptor and emission spectrum of the energy donor as well as the distance between the energy donor and acceptor. Herein, it was seen that the emission signal of PA was totally located within the covering region of CoOOH NSs and the emitted energy was completely absorbed by the nano-host. Thus, the fluorescence quenching of PA was observed.

Figure 5A recorded the fluorescence intensity changes of the aptamer PA in the presence of PSA at different concentrations, which clearly showed that fluorescence could be improved gradually due to the continuous addition of PSA species. Moreover, the emission changes versus the concentration of PSA were found to give a good linear relationship ( $R^2 = 0.9912$ ) in the range of 0.1 to 5 nM, and the limit of detection (LOD) was calculated to be 56.1 pM, according to the 3SD/slop approach. To explore the potential applications, a series of representative cations, anions, and biomolecules were used to evaluate the sensing properties of CoOOH NSs (Fig. 6). Compared with other interference analytes, PSA could be the only target to generate the green light with great selectivity.

## Conclusion

Current study is focused on the exploration of 2D materials in the field of catalysis and energy chemistry. Herein, this work developed its potential in the substrate for fluorescent sensing. Understanding and controlling its microstructure would extend its performance in a variety of aspects. In this way, we have constructed a novel fluorescence biosensor for the PSA detection by using CoOOH NSs as the

fluorescence quencher. Additionally, this CoOOH NSs also possesses a few merits including good biocompatibility, easy preparation and low cost. Therefore, it could be applied in the area of cell imaging, biomedical research, and other biological applications.

## Declarations

### Author Declarations

#### Funding (information that explains whether and by whom the research was supported)

Q. M. appreciates Natural Science Foundation of Guangdong Province, China (No. 2021A1515010324), Science and Technology Plan of Guangdong Province (No. 2020A0505100055), Guangzhou Science and Technology Plan (No. 202002030325)

#### Conflicts of interest/Competing interests (include appropriate disclosures)

The authors declare that non conflicts of interest

#### Ethics approval (include appropriate approvals or waivers)

This manuscript is not currently under consideration, in press or published elsewhere and is truthful original work without fabrication, fraud or plagiarism.

#### Consent to participate (include appropriate statements)

Not applicable.

#### Consent for publication (include appropriate statements)

Not applicable.

#### Availability of data and material (data transparency)

All data generated or analyzed during this study are included in this published article.

#### Code availability (software application or custom code)

Not applicable.

#### Authors' contributions (include all authors)

Junjie Chen: Writing - original draft

Xiangqian Li: Investigation

Xiaoqi Yu: Assisted with data collection and data analysis..

Qianming Wang: Supervision, writing and reviewing.

## References

1. Zhao R, Zhao L, Feng H, Chen X, Zhang H, Bai Y, Feng F, Shuang S (2021) A label-free fluorescent aptasensor based on HCR and G-quadruplex DNAzymes for the detection of prostate-specific antigen. *Analyst* 146(4):1340–1345
2. Li X, Wei L, Pan L, Yi Z, Wang X, Ye Z, Xiao L, Li H-W, Wang J (2018) Homogeneous Immunosorbent Assay Based on Single-Particle Enumeration Using Upconversion Nanoparticles for the Sensitive Detection of Cancer Biomarkers. *Anal Chem* 90(7):4807–4814
3. Pei HM, Zhu SY, Yang MH, Kong RM, Zheng YQ, Qu FL (2015) Graphene oxide quantum dots@silver core-shell nanocrystals as turn-on fluorescent nanoprobe for ultrasensitive detection of prostate specific antigen. *Biosens Bioelectron* 74:909–914
4. Soomro RA, Jawaid S, Zhang P, Han X, Hallam KR, Karakus S, Kilslioglu A, Xu B, Willander M (2021) NiWO<sub>4</sub>-induced partial oxidation of MXene for photo-electrochemical detection of prostate-specific antigen. *Sensor Actuat B-Chem* 328:129074
5. Chen JL, Tong P, Huang LT, Yu ZH, Tang DP (2019) Ti3C2 MXene nanosheet-based capacitance immunoassay with tyramine-enzyme repeats to detect prostate-specific antigen on interdigitated micro-comb electrode. *Electrochim Acta* 319:375–381
6. Shao K, Wang BR, Nie AX, Ye SY, Ma J, Li ZH, Lv ZC, Han HY (2018) Target-triggered signal-on ratiometric electrochemiluminescence sensing of PSA based on MOF/Au/G-quadruplex. *Biosens Bioelectron* 118:160–166
7. Bhardwaj SK, Sharma AL, Bhardwaj N, Kukkar M, Gill AAS, Kim KH, Deep A (2017) TCNQ-doped Cu-metal organic framework as a novel conductometric immunosensing platform for the quantification of prostate cancer antigen. *Sensor Actuat B-Chem* 240:10–17
8. You PY, Li FC, Liu MH, Chan YH (2019) Colorimetric and Fluorescent Dual-Mode Immunoassay Based on Plasmon-Enhanced Fluorescence of Polymer Dots for Detection of PSA in Whole Blood. *ACS Appl Mater Inter* 11(10):9841–9849
9. Zhao YT, Gao W, Ge XX, Li SQ, Du D, Yang HP (2019) CdTe@SiO<sub>2</sub> signal reporters-based fluorescent immunosensor for quantitative detection of prostate specific antigen. *Anal Chim Acta* 1057:44–50
10. Kong RM, Zhang XB, Ding L, Yang DS, Qu FL (2017) Label-free fluorescence turn-on aptasensor for prostate-specific antigen sensing based on aggregation-induced emission-silica nanospheres. *Anal Bioanal Chem* 409(24):5757–5765
11. Qu F, Ding YR, Lv XX, Xia L, You JM, Han WL (2019) Emissions of terbium metal-organic frameworks modulated by dispersive/agglomerated gold nanoparticles for the construction of prostate-specific antigen biosensor. *Anal Bioanal Chem* 411(17):3979–3988
12. Xu DD, Deng YL, Li CY, Lin Y, Tang HW (2017) Metal-enhanced fluorescent dye-doped silica nanoparticles and magnetic separation: A sensitive platform for one-step fluorescence detection of

prostate specific antigen. *Biosens Bioelectron* 87:881–887

13. Zhou Z, Wang XW, Zhang H, Huang HX, Sun LA, Ma L, Du YH, Pei CJ, Zhang QH, Li H, Ma LF, Gu L, Liu Z, Cheng L, Tan CL (2021) Activating Layered Metal Oxide Nanomaterials via Structural Engineering as Biodegradable Nanoagents for Photothermal Cancer Therapy. *Small* 17(12)
14. Yang Y, Cen Y, Deng WJ, Yu RQ, Chen TT, Chu X (2016) An aptasensor based on cobalt oxyhydroxide nanosheets for the detection of thrombin. *Anal Methods-UK* 8(39):7199–7203
15. Kong RM, Ding L, Wang ZJ, You JM, Qu FL (2015) A novel aptamer-functionalized MoS<sub>2</sub> nanosheet fluorescent biosensor for sensitive detection of prostate specific antigen. *Anal Bioanal Chem* 407(2):369–377
16. Lan LY, Chen DK, Yao Y, Peng XS, Wu J, Li YB, Ping JF, Ying YB (2018) Phase-Dependent Fluorescence Quenching Efficiency of MoS<sub>2</sub> Nanosheets and Their Applications in Multiplex Target Biosensing. *ACS Appl Mater Inter* 10(49):42009–42017
17. Peng XY, Zhang YL, Lu DT, Guo YJ, Guo SJ (2019) Ultrathin Ti<sub>3</sub>C<sub>2</sub> nanosheets based "off-on" fluorescent nanoprobe for rapid and sensitive detection of HPV infection. *Sensor Actuat B-Chem* 286:222–229
18. Wu T, Li X, Fu YQ, Ding XL, Li ZJ, Zhu GF, Fan J (2020) A highly sensitive and selective fluorescence biosensor for hepatitis C virus DNA detection based on delta-FeOOH and exonuclease III-assisted signal amplification. *Talanta* 209
19. Zhou H, Peng JB, Qiu XL, Gao YS, Lu LM, Wang WM (2017) beta-Ni(OH)<sub>2</sub> nanosheets: an effective sensing platform for constructing nucleic acid-based optical sensors. *J Mater Chem B* 5(35):7426–7432
20. Zhao MT, Wang YX, Ma QL, Huang Y, Zhang X, Ping JF, Zhang ZC, Lu QP, Yu YF, Xu H, Zhao YL, Zhang H (2015) Ultrathin 2D Metal-Organic Framework Nanosheets. *Adv Mater* 27(45):7372–7378
21. Liu JJ, Tang DS, Chen ZT, Yan XM, Zhong Z, Kang LT, Yao JN (2017) Chemical redox modulated fluorescence of nitrogen-doped graphene quantum dots for probing the activity of alkaline phosphatase. *Biosens Bioelectron* 94:271–277
22. Han QX, Yang H, Wen ST, Jiang HE, Wang L, Liu WS (2018) Selective and rapid detection of ascorbic acid by a cobalt oxyhydroxide-based two-photon fluorescent nano-platform. *Inorg Chem Front* 5(4):773–779
23. Saberi Z, Rezaei B, Faroukhpoor H, Ensafi AA (2018) A fluorometric aptasensor for methamphetamine based on fluorescence resonance energy transfer using cobalt oxyhydroxide nanosheets and carbon dots. *Microchim. Acta* 185(6)
24. Feng TT, Feng D, Shi W, Li XH, Ma HM (2012) A graphene oxide-peptide fluorescence sensor for proteolytically active prostate-specific antigen. *Mol Biosyst* 8(5):1441–1445
25. Gu JP, Li XQ, Zhou Z, Liu WQ, Li K, Gao JW, Zhao Y, Wang QM (2019) 2D MnO<sub>2</sub> nanosheets generated signal transduction with 0D carbon quantum dots: synthesis strategy, dual-mode behavior and glucose detection. *Nanoscale* 11(27):13058–13068

26. Dhenadhayalan N, Yadav K, Sriram MI, Lee HL, Lin KC (2017) Ultra-sensitive DNA sensing of a prostate-specific antigen based on 2D nanosheets in live cells. *Nanoscale* 9(33):12087–12095
27. Chen MJ, Ma CB, Yan Y, Zhao H (2019) A label-free fluorescence method based on terminal deoxynucleotidyl transferase and thioflavin T for detecting prostate-specific antigen. *Anal Bioanal Chem* 411(22):5779–5784
28. Zhou Z, Li B, Shen C, Wu D, Fan H, Zhao J, Li H, Zeng Z, Luo Z, Ma L, Tan C (2020) Metallic 1T Phase Enabling MoS<sub>2</sub> Nanodots as an Efficient Agent for Photoacoustic Imaging Guided Photothermal Therapy in the Near-Infrared-II Window. *Small* 16(43):2004173
29. Zhang H, Wang Z, Yang XQ, Li ZL, Sun LH, Ma JM, Jiang H (2019) The determination of alpha-glucosidase activity through a nano fluorescent sensor of F-PDA-CoOOH. *Anal Chim Acta* 1080:170–177
30. Wang CX, Pan CW, Wei ZT, Wei XR, Yang F, Mao LQ (2020) Bionanosensor based on N-doped graphene quantum dots coupled with CoOOH nanosheets and their application for in vivo analysis of ascorbic acid. *Anal Chim Acta* 1100:191–199
31. Liu SG, Luo D, Han L, Li NB, Luo HQ (2019) A hybrid material composed of guanine-rich single stranded DNA and cobalt(III) oxyhydroxide (CoOOH) nanosheets as a fluorescent probe for ascorbic acid via formation of a complex between G-quadruplex and thioflavin T. *Microchim. Acta* 186(3)
32. Zhang LM, Qin J, Yang Q, Wei SQ, Yang R (2019) Redox modulated fluorometric sensing of ascorbic acid by using a hybrid material composed of carbon dots and CoOOH nanosheets. *Microchim. Acta* 186(6)
33. Yang X, Long C, Tan Y, Wang Q (2021) Surface recognition strategy via ascorbic acid-triggered decomposition of boron nitride-loaded cobalt oxyhydroxide nanosheets. *Alloy Compd* 872
34. Tan CL, Zhang H (2015) Two-dimensional transition metal dichalcogenide nanosheet-based composites. *Chem Soc Rev* 44(9):2713–2731
35. Yu JF, Wang Q, O'Hare D, Sun LY (2017) Preparation of two dimensional layered double hydroxide nanosheets and their applications. *Chem Soc Rev* 46(19):5950–5974

## Figures

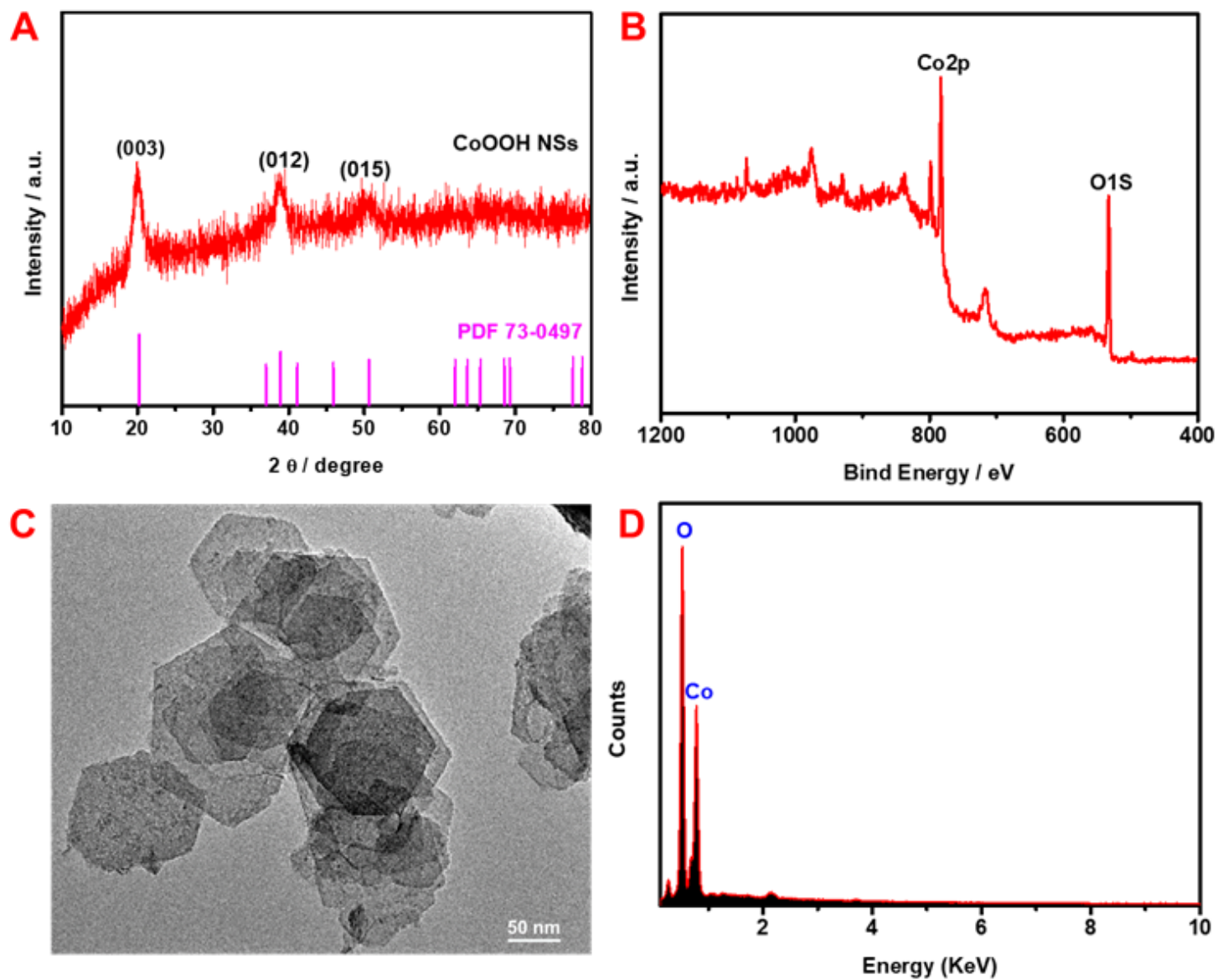


**Figure 1**

(A) XRD pattern, (B) XPS spectrum, (C) TEM image and (D) EDS of CoOOH NSs.

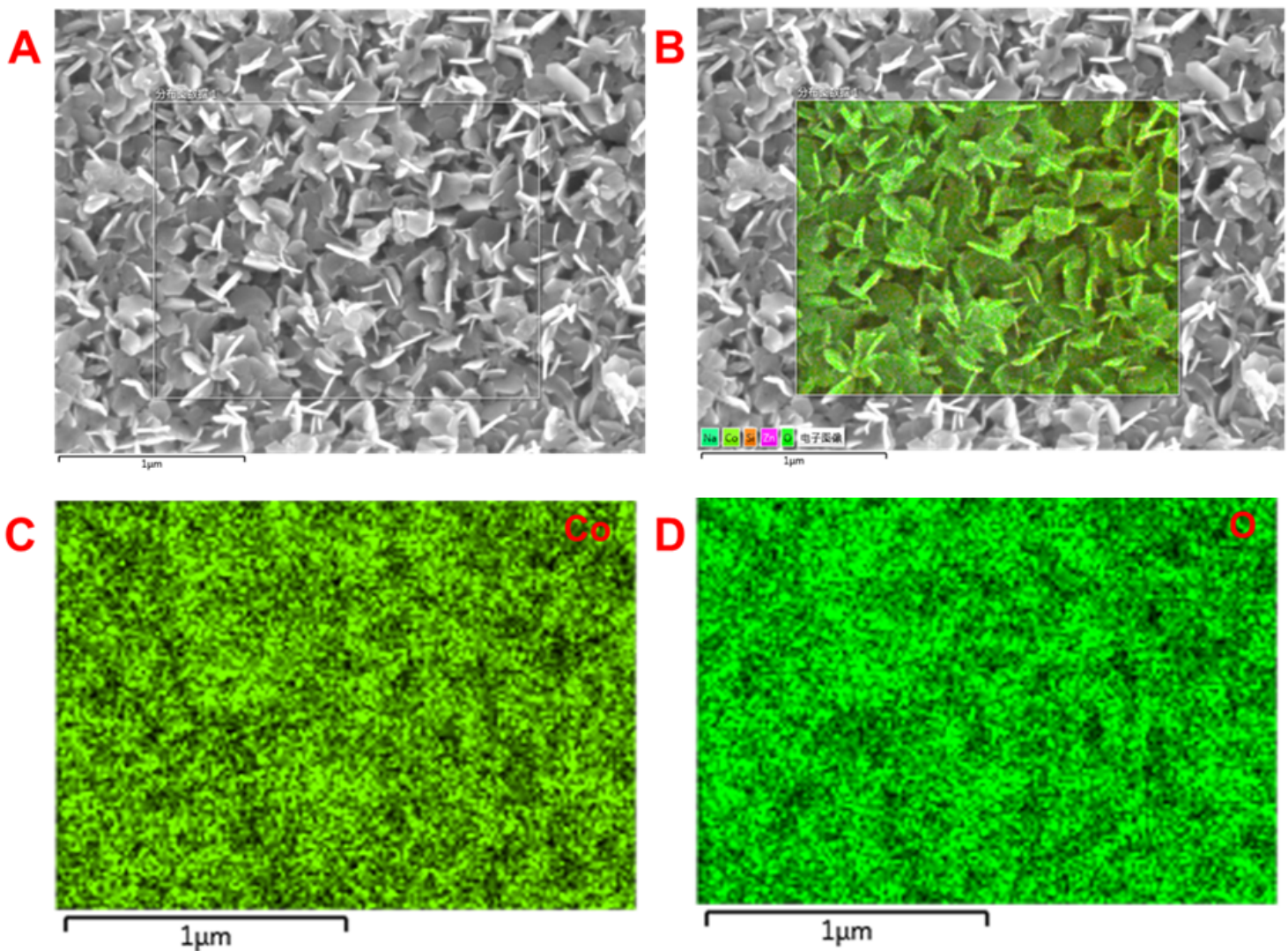


**Figure 2**

SEM and elemental mapping of CoOOH NSs.

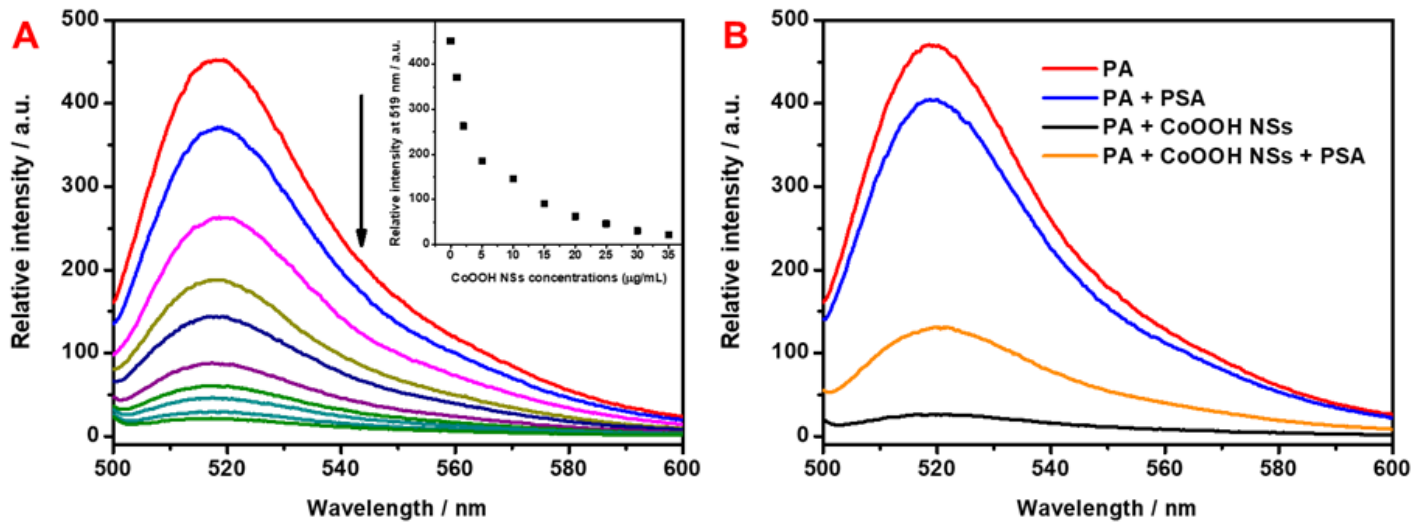


**Figure 3**

(A) Fluorescence spectra of PA (50 nM) upon addition of different concentrations CoOOH NSs (0-35  $\mu\text{g/mL}$ ). (B) Fluorescence spectra of PA (50 nM) and PA/PSA (50 nM/100nM) with or without CoOOH NSs.

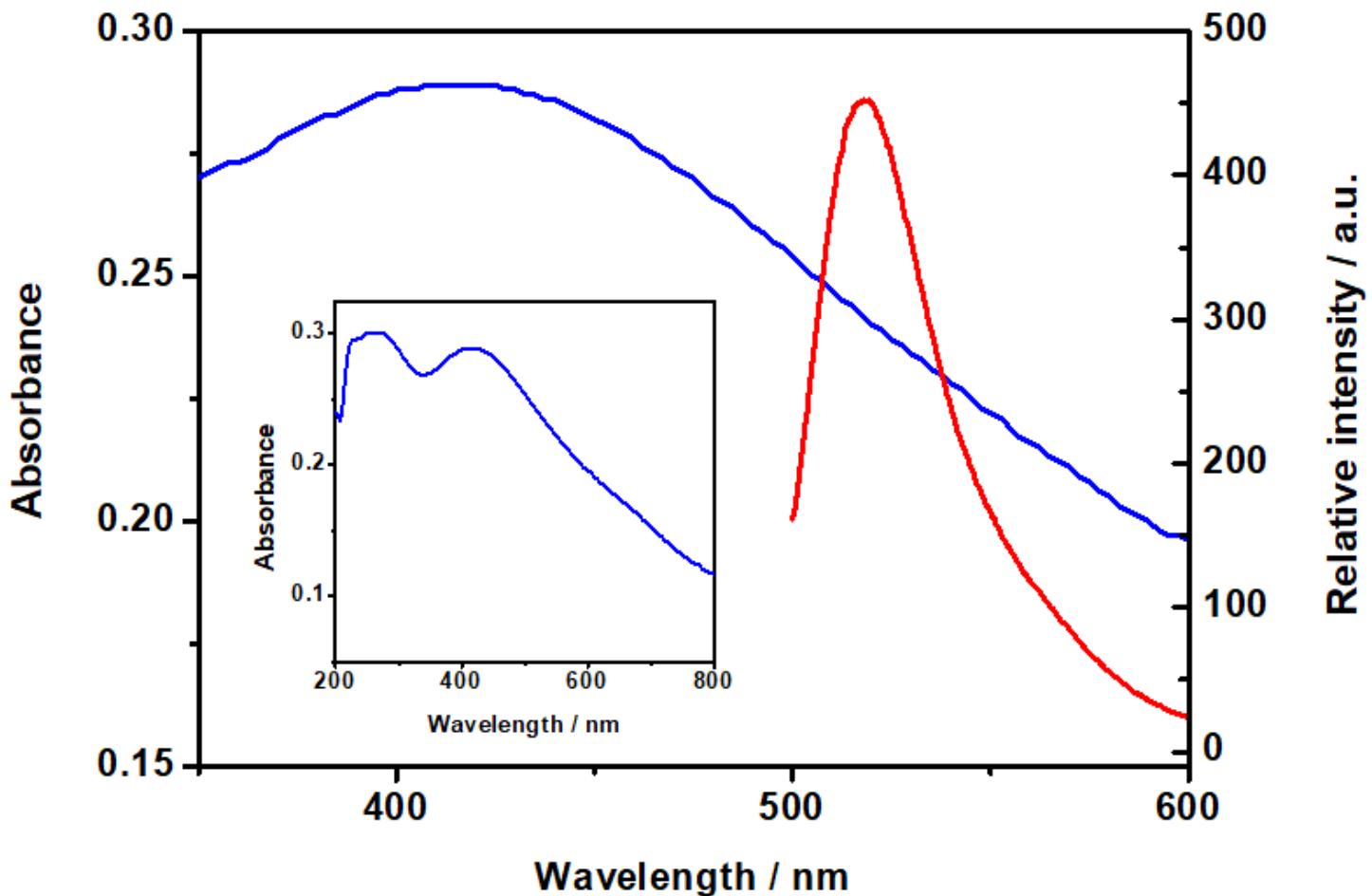


**Figure 4**

Absorption spectrum of CoOOH NSs and fluorescence spectrum of aptamer PA in pH 7.4 PBS (Inset: Absorption spectrum of CoOOH NSs at 200-800 nm).

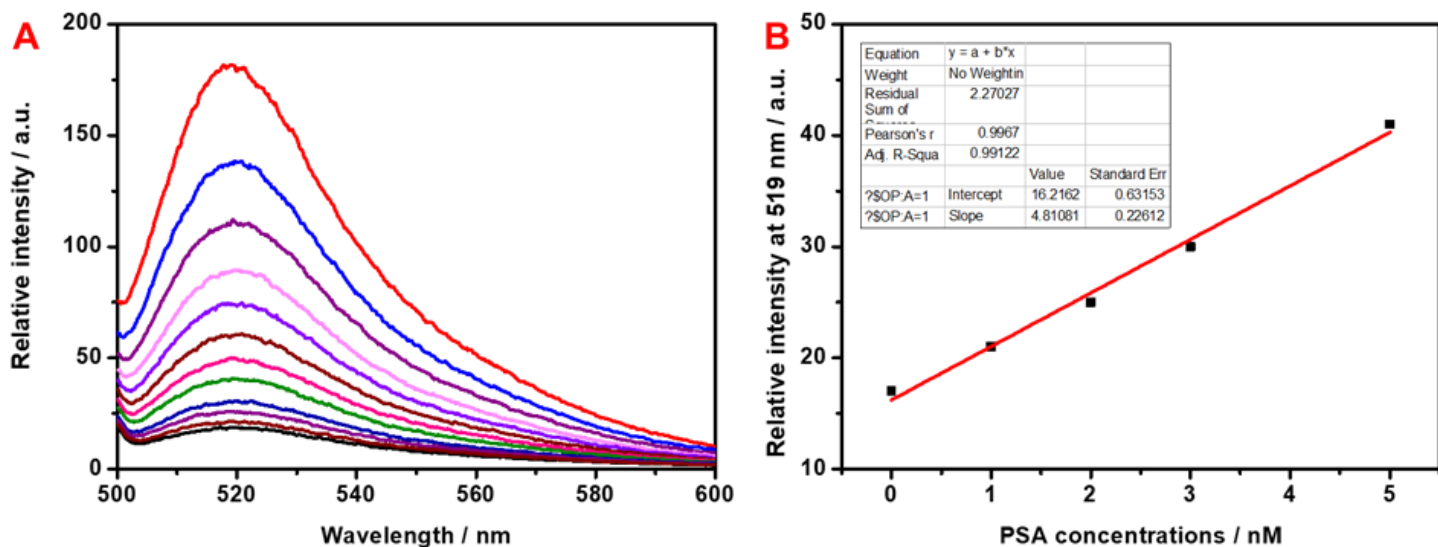


**Figure 5**

Detection performance of CoOOH NSs. (A) Fluorescence spectra for FAM-labeled aptamer (PA, 50 nM) under a series of concentrations of PSA (0, 1, 2, 3, 4, 5, 10, 15, 20, 25, 30, 35, 40, 45, 50, and 100 nM, respectively). (B) The linear of plot of the fluorescence intensity change at 519 nm as a function of PSA concentration.

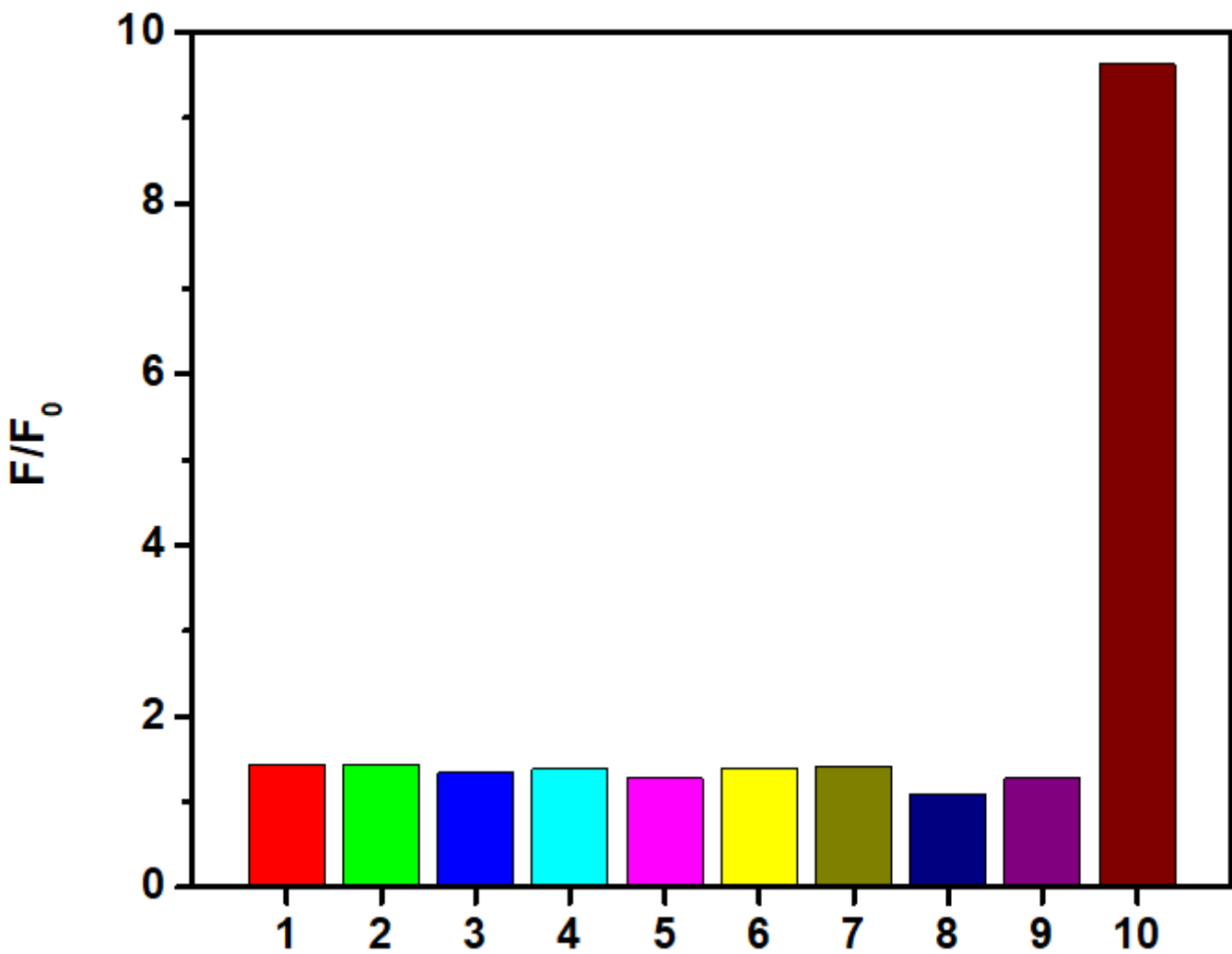


**Figure 6**

The selectivity of the CoOOH NSs based PSA biosensor, 1 CaCl<sub>2</sub>, 2 MgCl<sub>2</sub>, 3 ZnCl<sub>2</sub>, 4 BSA, 5 GSH, 6 Cys, 7 UA, 8 AA, 9 VB1 10 PSA.

## Supplementary Files

This is a list of supplementary files associated with this preprint. Click to download.

- supportinginformation.doc
- Scheme1.png